



HAL
open science

Phase transition in C 2O 4DND 4, 1/2D 2O : a coherent inelastic neutron scattering study

M. Krauzman, M. Debeau, R. Pick, M. Quilichini, P. Launois, F. Moussa

► To cite this version:

M. Krauzman, M. Debeau, R. Pick, M. Quilichini, P. Launois, et al.. Phase transition in C 2O 4DND 4, 1/2D 2O : a coherent inelastic neutron scattering study. Journal de Physique I, 1992, 2 (3), pp.329-351. 10.1051/jp1:1992146 . jpa-00246487

HAL Id: jpa-00246487

<https://hal.science/jpa-00246487>

Submitted on 4 Feb 2008

HAL is a multi-disciplinary open access archive for the deposit and dissemination of scientific research documents, whether they are published or not. The documents may come from teaching and research institutions in France or abroad, or from public or private research centers.

L'archive ouverte pluridisciplinaire **HAL**, est destinée au dépôt et à la diffusion de documents scientifiques de niveau recherche, publiés ou non, émanant des établissements d'enseignement et de recherche français ou étrangers, des laboratoires publics ou privés.

Classification
 Physics Abstracts
 64.60C — 64.70K

Phase transitions in $C_2O_4DND_4, \frac{1}{2}D_2O$: a coherent inelastic neutron scattering study

M. Krauzman⁽¹⁾, M. Debeau⁽¹⁾, R.M. Pick⁽¹⁾, M. Quilichini⁽²⁾, P. Launois⁽²⁾
 and F. Moussa⁽²⁾

⁽¹⁾ Département de Recherches Physiques(*), Université P. et M. Curie, 75252 Paris Cedex 05, France

⁽²⁾ Laboratoire Léon Brillouin(*), CEN-Saclay, 91191 Gif-sur-Yvette Cedex, France

(Received 26 September 1991, accepted in final form 7 November 1991)

Résumé. — On étudie la dynamique de basse fréquence liée à la transition de phase du deuxième ordre de l'oxalate d'ammonium deutéré, par diffusion cohérente inélastique des neutrons. Cette transition est ferroélastique à pression atmosphérique, et conduit à une phase modulée à 5kbar. Dans les deux cas, les expériences montrent que le mécanisme de la transition est le couplage entre les phonons TA qui se propagent suivant c^* et sont polarisés suivant a et un mode de réorientations d'une famille d'ions ND_4^+ . Ces derniers sont couplés par des interactions de type ANNNI qui dépendent de la pression. De faibles changements des valeurs des paramètres entre les deux pressions suffisent à expliquer des comportements statiques et dynamiques différents.

Abstract. — The low frequency dynamics related to the second order transition which takes place in ammonium deuterated oxalate has been investigated by coherent inelastic neutron scattering. This transition leads to a ferroelastic phase at zero pressure and to an incommensurate phase at 5kbar. At both pressures, our experiments show that the coupling between a reorientation motion of one family of ND_4^+ ions and the TA phonons propagating along c^* and polarized along a drives the transition, the ND_4^+ being coupled through a pressure dependent ANNNI model. Weak changes in the parameters explain the changes with pressure of the static and dynamical properties of the transition.

1. Introduction.

This paper reports on the first inelastic neutron scattering experiments performed on ammonium deuterium oxalate $C_2O_4DND_4, 1/2D_2O$ (in short AHOD). This crystal, as well as its non deuterated analog, AHO, has been already studied by various techniques. X rays measurements

(*) U.A. 71.

(*) Laboratoire Commun CEA-CNRS.

[1,2] revealed that in the room temperature phase, (phase I, space group Pmnb (D_{2h}^{16}) with $Z = 8$), the NH_4^+ ions form two distinct families, both located on the mirror planes, one of these families being disordered. At zero pressure, AHO and AHOD undergo a second order, equitranslational, transition which leads to a $P1\frac{2_1}{n}1$ (C_{2h}^5) structure (phase II) [3]. A Brillouin scattering experiment proved that the elastic constant C_{55} dramatically decreases in the vicinity of this phase transition, indicating a ferroelastic character [4].

Raman scattering experiments [5,6] revealed, in the vicinity of this transition, the existence of a central peak visible in the B_{2g} (ac) geometry, the intensity of which increased while its linewidth decreased close to the transition. These Brillouin and Raman experiments were interpreted as the result of a strong coupling between the NH_4^+ ordering process, and the e_5 shear deformation. Indeed, each disordered NH_4^+ ion has two possible orientations, symmetric with respect to the mirror plane. These two orientations can be represented by the two values of a one half pseudospin, and one of the linear combinations of the four pseudospins existing in the unit cell generates a spin variable with the B_{2g} symmetry. This variable displays diffusive dynamics, characterized by the relaxation mode detected in our Raman experiments. This mode should, by itself, freeze at a temperature T_0 which, in AHO, turned out to be around 40 K. Nevertheless, this variable is linearly coupled to the e_5 deformation, and this coupling is strong enough to push the transition temperature up to $T_c = 146$ K, temperature at which the elastic constant goes to zero. These Raman experiments enabled one of us [5] to analyse the NH_4^+ individual reorientational dynamics. It was found that this dynamics could be described by a Markovian process, characterized by a mean life time, τ , in a given orientation, which, in phase I, was simply governed by an Arrhenius process

$$\tau = \tau_0 \exp(\beta V_0) \quad (1)$$

Another set of Raman scattering experiments were also performed under hydrostatic pressure [5,7]. It showed that, below a critical temperature $T_c = 146$ K, and above a critical pressure $P_c = 2.6$ kbar, the second order phase transition leads to a new phase, called phase III; by decreasing further the temperature, at constant pressure, phase II was recovered through a first order phase III - phase II transition. The analysis of these experiments suggested [6] that phase III could be incommensurate, characterized by a wave vector q_0 which would depend on pressure but not on temperature.

This suggestion was confirmed by X ray [8] and elastic neutron experiments [9]: q_0 was found to remain parallel to c^* and to vary, for AHOD, from at most $0.06 c^*$ at $P = 2.8$ kbar to at least $0.24 c^*$ at 8 kbar. From the combined analysis of the ultrasonic and Brillouin measurements [4,10], and of the Raman data, it was proposed [7] that the phase I - II transition below P_c , and the phase I - III transition above P_c could be driven by the same mechanism, namely a strong coupling between the pseudospin ordering and a local deformation: this deformation develops coherently either as a TA phonon propagating along c^* and polarized along a ($P > P_c$) or as its $q = 0$ limit, i.e. an e_5 deformation (for $P < P_c$).

The present inelastic neutron experiments were undertaken in order to check the validity of such a prediction. The dynamical consequences of a bilinear coupling between a phonon system and a pseudospin system are known, from a general point of view, since the pioneering work of Yamada *et al.* [11]. They showed that the same mechanism leads to two very different situations close to the transition depending on the value of $\omega_{ph}\tau$ where τ is the individual residence time defined above (Eq. (1)) and ω_{ph} is the bare frequency of the modulation which will eventually freeze below the phase transition. Our Raman experiments suggested that both above and below P_c , an $\omega_{ph}\tau \ll 1$ situation would prevail. The present work shows that,

indeed, the proposed mechanism drives the transition both below and above P_c , but that, at least at 5 kbar, and quite presumably above this pressure, one deals with an $\omega_{ph}\tau \gtrsim 1$ regime.

The present paper is organized as follows: we briefly review, in section 2, the bilinear phonon-pseudospin coupling theory to emphasize the shape of the phonon dynamical response function in the two cases $\omega_{ph}\tau < 1$ and $\omega_{ph}\tau > 1$, and the wave vector dependence of the linewidths of this response function. Section 3 describes the form of the interaction energy between the pseudospins that we have been using for analyzing our neutron data. In section 4, we give some details on the experimental set up, and on the method we have used to analyze the data in order to extract parameters which should reproduce the principal features of the phonon response function. These parameters are analyzed in section 5, first on a qualitative basis, secondly on a quantitative one which shows a fairly reasonable agreement with the model developed in sections 2 and 3. Finally section 6 summarizes our result, and compares the consequences of the interaction energy of section 3 with that of an alternative model proposed to describe the phase diagram of AHOD.

2. Description of the model.

In this section, we shall recall the principal properties of the dynamical model we are going to use for the analysis of our neutron inelastic scattering data.

The structural data on phases I and II of Küppers *et al.* [2,3] show that the oxalate ions $C_2O_4H^-$ lie in planes perpendicular to the crystallographic c axis, roughly located at $z = \frac{1}{4}$ and $z = \frac{3}{4}$; they form chains approximately parallel to the b axis, and strongly coupled in these planes. The two families of NH_4^+ ions are located in the vicinity of the planes $z = 0$ and $z = \frac{1}{2}$, and each NH_4^+ lie on one of the mirror planes at $x = \frac{1}{4}$ or $x = \frac{3}{4}$. These ions act as cog-wheels between neighbouring $C_2O_4H^-$ planes, and one must conclude from the various experiments so far performed [4-9] that this cog-wheel motion can only take the form of a relative glide of two neighbouring planes in a direction parallel to the a axis. Such a motion can be viewed as a sum of transverse acoustic phonons, propagating along c^* and polarized along a .

In view of the analysis of our experimental data, which have been collected on phonons propagating and polarized in the (010) plane, we shall describe here a dynamical model valid not only for the TA phonons propagating along c^* and polarized along a , but for any pseudo TA phonons propagating and polarized in this plane.

The corresponding phonon free energy is:

$$F_{ph} = \frac{1}{2} \sum_{\mathbf{q}} \omega^2(\mathbf{q}) Q(\mathbf{q}) Q(-\mathbf{q}) \quad (2)$$

where \mathbf{q} is restricted to the (010) plane and $Q(\mathbf{q})$ is the TA phonon normal coordinate. Due to the special symmetry properties of the non symmorphic Pmnb space group [12], all the representations are degenerate, in this plane, at the zone boundary, so that $\omega^2(\mathbf{q})$ can fairly well be represented, for all the wave vectors of interest by:

$$\omega^2(\mathbf{q}) = v^2(\hat{\mathbf{q}}) q^2 \quad (3)$$

where $v(\hat{\mathbf{q}})$ is the speed of sound in the $\mathbf{q} \rightarrow 0$ limit for \mathbf{q} parallel to the unit vector $\hat{\mathbf{q}}$.

The four equivalent sites on which the disordered NH_4^+ ions are located have coordinates [1]:

$$\begin{aligned} (1) \quad \frac{1}{4}, +\eta, +\varepsilon & \quad (3) = \frac{1}{4}, +\eta + \frac{1}{2}, -\varepsilon + \frac{1}{2} \\ (2) \quad \frac{3}{4}, -\eta, -\varepsilon & \quad (4) = \frac{3}{4}, -\eta + \frac{1}{2}, +\varepsilon + \frac{1}{2} \end{aligned} \quad (4)$$

where η is close to $\frac{1}{4}$ and $\varepsilon \ll 1$.

If σ_i^L ($i = 1-4$) is the pseudospin variable which describes the NH_4^+ orientation disorder at the site i of the L^{th} cell of the crystal, σ_i^L transforms, under the mirror plane operation which leaves that site invariant, as the A'' (odd) representation of the site symmetry group. Let us define $\sigma_i(\mathbf{q})$ as the Fourier transform of σ_i^L :

$$\sigma_i(\mathbf{q}) = \frac{1}{\sqrt{N}} \sum_L \sigma_i^L e^{i\mathbf{q} \cdot (\mathbf{R}_L + \mathbf{t}_i)} \quad (5)$$

where:

$$\mathbf{t}_1 = 0, \quad \mathbf{t}_2 = \frac{\mathbf{a}}{2}, \quad \mathbf{t}_3 = \frac{\mathbf{c}}{2} \quad \text{and} \quad \mathbf{t}_4 = \frac{\mathbf{a} + \mathbf{c}}{2} \quad (6)$$

Let us furthermore define:

$$\begin{aligned} \sigma_a(\mathbf{q}) &= \frac{1}{2} [\sigma_1(\mathbf{q}) + \sigma_2(\mathbf{q}) + \sigma_3(\mathbf{q}) + \sigma_4(\mathbf{q})] \\ \sigma_b(\mathbf{q}) &= \frac{1}{2} [\sigma_1(\mathbf{q}) + \sigma_2(\mathbf{q}) - \sigma_3(\mathbf{q}) - \sigma_4(\mathbf{q})] \\ \sigma_c(\mathbf{q}) &= \frac{1}{2} [\sigma_1(\mathbf{q}) - \sigma_2(\mathbf{q}) + \sigma_3(\mathbf{q}) - \sigma_4(\mathbf{q})] \\ \sigma_d(\mathbf{q}) &= \frac{1}{2} [\sigma_1(\mathbf{q}) - \sigma_2(\mathbf{q}) - \sigma_3(\mathbf{q}) + \sigma_4(\mathbf{q})]. \end{aligned} \quad (7)$$

One easily verifies [12] that $\sigma_d(\mathbf{q})$ transforms under the space group operations, as the B_{2g} representation for $\mathbf{q} = 0$, as the τ_4 representation for $\mathbf{q} \parallel \mathbf{c}^*$ and as the τ_3 representation for $\mathbf{q} \parallel \mathbf{a}^*$, while $\sigma_a(\mathbf{q})$ transforms for the same vectors, respectively as B_{3u} , τ_4 and τ_1 . Following [7], the free energy related to the $\sigma_d(\mathbf{q})$ components of the pseudospins is, in the vicinity of the phase transition:

$$F_{\text{ps}} = \frac{1}{2} \sum_{\mathbf{q}} [k_B T - J_d(\mathbf{q})] \sigma_d(\mathbf{q}) \sigma_d(-\mathbf{q}) + \text{higher order terms} \quad (8)$$

where k_B is the Boltzman constant, and $J_d(\mathbf{q})$ the interaction energy constant, the \mathbf{q} dependence of which will be discussed in section 3.

Finally, $\sigma_d(\mathbf{q})$ and the pseudo TA phonon with the same \mathbf{q} , belong to the same representation, and are thus bilinearly coupled, this coupling describing, in some sense, the cog-wheel aspect of the problem. As $Q(\mathbf{q})$ represents, in the Fourier space, a quasi-homogenous displacement, the corresponding part of the free energy must be written as:

$$F_c = \frac{1}{2} \sum_{\mathbf{q}} i \left(\hat{\mathbf{u}}(\hat{\mathbf{q}}) \cdot \overline{\overline{\mathbf{d}}} \cdot \mathbf{q} \right) [Q(\mathbf{q}) \sigma_d(-\mathbf{q}) - Q(-\mathbf{q}) \sigma_d(\mathbf{q})] \quad (9)$$

where $\overline{\overline{\mathbf{d}}}$ is a second rank tensor and $\hat{\mathbf{u}}(\hat{\mathbf{q}})$ is the displacement vector (normalized to unity) associated with $Q(\mathbf{q})$; as in the case of the pseudo TA phonon dispersion curve, one expects

that the algebraic form of equation (9) holds up to the Brillouin zone boundary, i.e. that it will not be necessary to introduce any other \mathbf{q} dependence in \bar{d} . The total free energy is the sum of equations (2), (8) and (9) and the corresponding equations of motions for $Q(\mathbf{q})$ and $\sigma_d(\mathbf{q})$ may be deduced from:

$$\frac{\partial F}{\partial Q(-\mathbf{q})} = \omega^2 Q(\mathbf{q}) \quad \frac{\partial F}{\partial \sigma_d(-\mathbf{q})} = i\omega\tau k_B T \sigma_d(\mathbf{q}). \quad (10)$$

In the high temperature phase I, we can, in the mean field approximation, neglect the higher order terms of equation (8), and we shall neglect any intrinsic phonon damping. The phonon response function $\langle Q(\mathbf{q}, \omega) Q(\mathbf{q}, \omega)^* \rangle$ is then given by

$$\langle Q(\mathbf{q}, \omega) Q(\mathbf{q}, \omega)^* \rangle = [1 + n(\omega)] \text{Im} \frac{1}{\omega^2(\mathbf{q}) - \omega^2 - \frac{(\hat{\mathbf{u}}(\hat{\mathbf{q}}) \cdot \bar{d} \cdot \mathbf{q})^2}{k_B T - J_d(\mathbf{q}) - i\omega\tau k_B T}} \quad (11)$$

where $n(\omega)$ is the usual Bose-Einstein factor.

In the following, $\hat{\mathbf{q}}$ will remain parallel either to \mathbf{a}^* or to \mathbf{c}^* . Then $\hat{\mathbf{u}}(\hat{\mathbf{q}})$ is the unit vector of the (010) plane perpendicular to $\hat{\mathbf{q}}$, \bar{d} is limited to its xz component, and one can write, to simplify:

$$d \equiv \hat{\mathbf{x}} \cdot \bar{d} \cdot \hat{\mathbf{z}} \equiv \hat{\mathbf{z}} \cdot \bar{d} \cdot \hat{\mathbf{x}}. \quad (12a)$$

Similarly, for these two propagation directions:

$$v(\hat{\mathbf{q}}) \equiv v_o = \sqrt{\frac{C_{55}}{\rho}} \quad (12b)$$

where C_{55} is the elastic constant relative to the e_5 shear deformation and ρ the mass density. Finally, it is convenient to write:

$$J_d(\mathbf{q}) = \kappa_B T_d(\mathbf{q}). \quad (12c)$$

Inserting equations (12a, b and c) into equation (11), and admitting, as will be the case, that $T_d(\mathbf{q})$ has its maximum for $\mathbf{q} = \mathbf{q}_o$, where \mathbf{q}_o is along a symmetry axis of the (010) plane, the transition temperature is given by:

$$v_o^2 - \frac{d^2}{k_B (T_c - T_d(\mathbf{q}))} = 0. \quad (13)$$

The general shape of the response function (Eq. (11)) has been already discussed e.g. in the original paper of Yamada *et al.* [11]. It is nevertheless worth while recalling here the main effects which are expected to appear in the present case which is characterized by two specific aspects:

a) the pseudospins couple to an acoustic phonon, and \mathbf{q}_o may be equal to zero ($P < P_o$ case).

b) The coupling is very strong for, in the hydrogenated case, at $P = 0$ kbar, the transition temperature is increased from $T_o \simeq 40$ K to $T_c = 146$ K, and the same orders of magnitude are expected to be found here. $1 - \frac{T_d(\mathbf{q})}{T}$ will thus be, in the whole temperature range, of the

order of unity (always larger than $\sim \frac{1}{2}$) and it is convenient to rewrite equation (11) under the form:

$$\langle Q(\mathbf{q}, \omega) Q(\mathbf{q}, \omega)^* \rangle = (1 + n(\omega)) \text{Im} \frac{1}{v_0^2 q^2 - \frac{d^2 q^2}{k_B T \left(1 - \frac{T_d(\mathbf{q})}{T} - i\omega\tau\right)} - \omega^2} \quad (14a)$$

$$= (1 + n(\omega)) \text{Im} \frac{1}{D(\mathbf{q}, \omega, T, \tau)} \quad (14b)$$

and to discuss the shape of the spectrum in two extreme cases.

a) q and τ are such that $v_0 q \tau \ll 1$.

$$D(\mathbf{q}, \omega, T, \tau) \sim \left(v_0^2 - \frac{d^2}{k_B [T - T_d(\mathbf{q})]} \right) q^2 - i\omega \frac{d^2 k_B T \tau}{[k_B [T - T_d(\mathbf{q})]]^2} q^2 - \omega^2 \quad (15)$$

$D(\mathbf{q}, \omega, T, \tau)$ represents, for each \mathbf{q} , a phonon, the frequency of which decreases with temperature, (and will, eventually go to zero for $T = T_c$ and $\mathbf{q} = \mathbf{q}_0$) while its linewidth, which is the coefficient of $i\omega$, increases. (The denominator $(T - T_d(\mathbf{q}))^2$ decreases with T , while the residence time τ increases enough, for $T\tau$ to increase when lowering T).

Furthermore, at each temperature, this linewidth varies as q^2 , as long as the $v_0 q \tau \ll 1$ approximation remains valid, this damping remaining relatively modest (see b)

b) $v_0 q \tau \gg 1$

$D(\mathbf{q}, \omega, T, \tau)$ may now be approximated, in the vicinity of $\omega = v_0 q$, by

$$D(\mathbf{q}, \omega, T, \tau) = \left(v_0^2 - \frac{d^2}{k_B [T - T_d(\mathbf{q})]} \left[\frac{[T - T_d(\mathbf{q})]}{v_0 q \tau T} \right]^2 \right) q^2 - \frac{id^2 q^2}{k_B T \omega \tau} - \omega^2 \quad (16a)$$

which shows that the phonon frequency practically does not change from its high temperature value, $v_0 q$. The phonon linewidth can thus be approximated by

$$\Gamma_{(\text{HWHM})} = \frac{d^2}{2v_0^2 k_B T \tau} \quad (16b)$$

indicating a q -independent linewidth which might decrease with decreasing temperature, and is always much larger than the value obtained in a).

Nevertheless, in the vicinity of $\omega = 0$, $\omega \tau \ll 1$ and one must write:

$$D(\mathbf{q}, \omega, T, \tau) \simeq \left\{ \left[v_0^2 - \frac{d^2}{k_B [T - T_d(\mathbf{q})]} \right] - i\omega \frac{d^2 k_B T \tau}{[k_B [T - T_d(\mathbf{q})]]^2} \right\} q^2 \quad (17)$$

This represents a Lorentzian central peak, the intensity of which diverges for $\mathbf{q} = \mathbf{q}_0$, $T = T_c$, while its width decreases (critical narrowing effect).

In summary, through their coupling to the pseudospin diffusive dynamics, the phonons always become damped (or acquire an extra damping if they were already damped) and the wave vector dependence of this damping changes according to the regime. Nevertheless, the main effect of the pseudospin ordering is the appearance, in addition to the normal phonon resonance, either of soft modes on some part of the acoustic phonon branch or of a central

peak. This was briefly discussed by Rowe *et al.* [13], in another context, and making use of a partly different model.

As we shall see in section 5, our experiments have revealed both types of behaviour. At zero pressure, we shall be in case a) for some of the considered wave vectors, both because $q_0 = 0$ and because τ is relatively short. Conversely, at 5 kbar, q_0 is finite, and τ has, at each temperature, a larger value than for $P = 0$. All our experiments will thus be characteristic either of case b), or of an intermediate case more reminiscent of case b) than of case a).

3. A model for the pseudospin interaction energy.

A very important feature of the AHOD structure is the quite short value of the lattice parameter c with respect to both a and b . For instance, at room temperature, we have found, at zero pressure

$$a = 12.3 \text{ \AA} \quad b = 11.3 \text{ \AA} \quad c = 6.9 \text{ \AA},$$

values quite similar to those obtained by Küppers [2] for AHO. Let us assume that the interaction between two ND_4^+ pseudospins can be monitored by the relative distance between their N atoms and, for the sake of simplicity⁽¹⁾, that ε (see Eq. (4)) is equal to zero. Then the four distances $\left| \frac{a}{2} + \frac{b}{2} \right|$, $\left| \frac{c}{2} + \frac{a}{2} \right|$, $\left| \frac{c}{2} + \frac{b}{2} \right|$ and $|c|$ turn out to be approximately the same. They

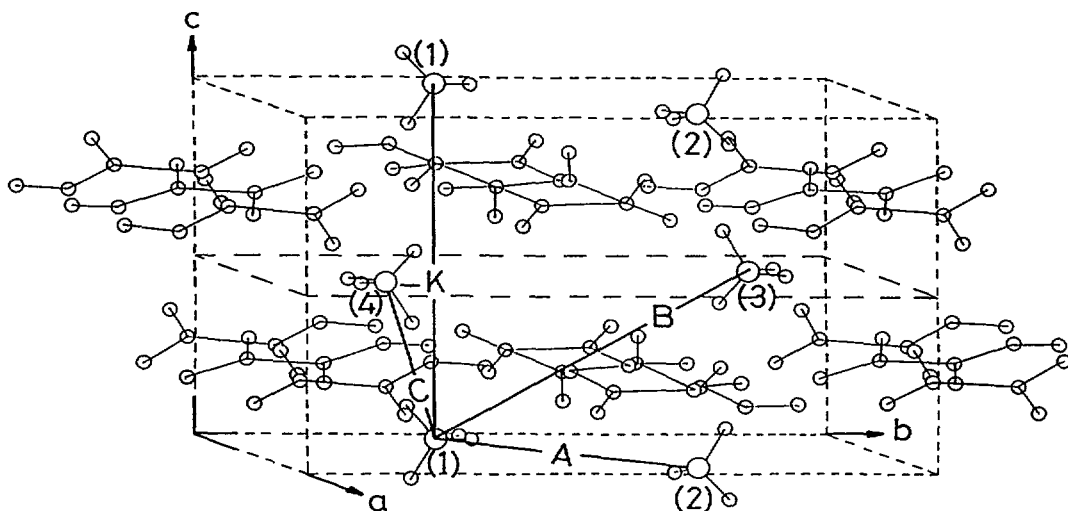


Fig. 1. — The four types of interactions. Only the interaction between pseudospin (1) and: pseudospin (2) differing by $\sim \frac{a+b}{2}$, (A type); pseudospin (3) differing by $\sim \frac{b+c}{2}$, (B type); pseudospin (4) differing by $\sim \frac{a+c}{2}$, (C type); pseudospin (1) differing by c , (K type) are shown here, while, in the actual calculation, all the + and - signs, their possible non equivalence, and all the interactions generated by the space group operations have been taken into account.

⁽¹⁾ This approximation has not been made in actually computing $J_d(q)$.

represent respectively the distances between one given pseudospin and

– its four nearest neighbours (see Fig. 1) located in the plane perpendicular to c with the same value for z ;

– its four nearest neighbours, in each of the two planes, with z differing by $\pm \frac{c}{2}$;

– its nearest neighbour, in each of the two planes, with z differing by $\pm c$.

Furthermore, these distances are clearly smaller than any other N-N distance between disordered ND_4^+ ions.

A lengthy but straightforward calculation shows that, when limiting the interactions of one pseudospin to the different pseudospins enumerated above, for \mathbf{q} parallel to the (010) plane, one gets, using equations (5) and (7) to transform the pseudospin interaction energy into Fourier space variables:

$$J_d(\mathbf{q}) = -A \cos X - B \cos Z + C \cos X \cos Z - K \cos 2Z \quad (18)$$

with:

$$X = \mathbf{q} \cdot \frac{\mathbf{a}}{2} \quad Z = \mathbf{q} \cdot \frac{\mathbf{c}}{2}. \quad (19)$$

In this expression:

A is the sum of the interaction constants between one pseudospin and its four nearest neighbours which belong to the plane with the same value of z . (Interaction between pseudospins (1) and (2) or pseudospins (3) and (4));

B is the sum of the interaction constants between one pseudospin and its four nearest neighbours which are in the same mirror plane and in planes differing by $\pm \frac{c}{2}$ (pseudospins (1) and (3) or pseudospins (2) and (4));

C is the same sum for the four pseudospins which belong to different mirror planes, with z differing by $\pm \frac{c}{2}$ (pseudospins (1) and (4) or pseudospins (2) and (3));

Finally, $\frac{-K}{4}$ is the interaction constant between one pseudospin and its nearest neighbour with z differing by c or $-c$.

Let us briefly comment on equation (18) and its physical meaning. First, for $P = 0$ kbar, the phase transition is ferroelastic, which means that the maximum of $J_d(\mathbf{q})$ takes place at $\mathbf{q} = 0$. This implies that:

$$C - A > 0; C - B > 4K > 0. \quad (20)$$

Conversely, for $P > P_c$, the phase transition takes place for $\mathbf{q} = \mathbf{q}_0$ where \mathbf{q}_0 is parallel to \mathbf{c}^* . This is possible only if:

$$C - A > 0; 4K > C - B > 0. \quad (21)$$

Secondly, for \mathbf{q} parallel to \mathbf{a}^* , $Z = 0$ so that the dispersion of $J_d(\mathbf{q})$ is only related to $C - A$. Similarly, for \mathbf{q} parallel to \mathbf{c}^* , $J_d(\mathbf{q})$ reduces to:

$$J_d(\mathbf{q}) = -C + (C - A) + (C - B) \cos Z - K \cos 2Z \quad \mathbf{q} // \mathbf{c}^*. \quad (22)$$

This means that the four effective coefficients of the theory are $C - A$, which describes the dispersion along \mathbf{a}^* , C , and finally $C - B$ and K which describe the dispersion along \mathbf{c}^* . It is the competition between the values of these two last parameters which will decide for a ferroelastic or an incommensurate low temperature phase (cf. Eq. (22)).

The preceding results have an obvious meaning. What has been developed in this section is an ANNNI model [14] with competing interactions between the nearest and the next nearest

planes: the nearest plane interaction is of the "ferro" type ($C - B > 0$) and the next nearest interaction of the "antiferro" type ($-K < 0$). One expects that pressure influences the ratio $(C - B)/4$ K, which is not unlikely because the lattice is rather soft along the c axis ($C_{33}/C_{11} \sim 0.35$, $C_{33}/C_{22} \sim 0.20$ [10]). The experimental evidence that the incommensurate phase exists only above a critical pressure P_c implies that this ratio decreases with increasing pressure. Due to the coupling with the TA phonon, the dynamics we are going to probe, in the following, will be that of a compressible ANNNI model.

In equation (18), the four interaction constants A , B , C and K have been introduced on a phenomenological basis. They represent, in fact, physical effects which have, at least, two different origins. First, each disordered ND_4^+ ion is in a general lattice position for all orientations, and thus has no reason to fully keep its tetrahedral symmetry. Indeed, a small dielectric signal related to the ND_4^+ reorientation dynamics has been detected by Albers *et al.* [15], (see Sect. 6) which indicates that each pseudospin orientation is related to a weak dipole moment. This results in a direct interaction between the pseudospins. A second and no less important origin is related to a direct interaction (Van der Waals, H bonding...) between a ND_4^+ ion and the neighbour oxalate ions. Eliminating the relative motion between these two types of ions leads to an effective interaction between pseudospins which is unfortunately very difficult to estimate.

4. Experiments.

4.1 DATA COLLECTION. — Inelastic neutron scattering experiments were performed at the ORPHEE Reactor (L.L.B., Saclay) with the triple axes spectrometer 4F1 located on a cold source. The sample was mounted either in a closed cycle displax cryostat or in a high pressure cell, for measurements at atmospheric pressure and at 5 kbar respectively. Data were taken as a function of temperature with a 0.1 K stability. Constant $k_i = 1.55 \text{ \AA}^{-1}$ scans allowed us to measure phonons in neutron energy gain with a flat analyser.

Both monochromator (vertically bent) and analyser were of pyrolytic graphite (PG(002)). A beryllium filter was used on incident k_i to avoid second order contamination. Horizontal collimations on incoming and outgoing neutrons were such that, for most of the data, the energy resolution was $\simeq 0.04$ THz. (The mosaic spread of the sample was approximately of $24'$). In order to measure the dispersion curves of the transverse acoustic modes which correspond (for $q \rightarrow 0$) to the C_{55} elastic constant, the sample was oriented with a scattering plane defined by a^* and c^* . At atmospheric pressure, we also performed one measurement in the (100) scattering plane. This allowed us to study the transverse acoustic mode which propagates along c^* and is polarized along b , a mode uncoupled to all the spin variables.

4.2 SPECTRAL PROFILE ANALYSIS. — Each spectral profile was analysed with the help of programs existing at the L.L.B. They are able to describe a profile as a sum of damped oscillators and of Lorentzian curves centered around a given frequency. As a consequence of the analysis performed in section 2, the spectrum was considered to be the sum of three separate terms:

a) The dynamical response of a damped oscillator: as usual, this function was described by:

$$S_{ph}(\mathbf{Q}, \omega) = (1 + n(\omega)) \text{Im} \left(\frac{F^2(\mathbf{Q})}{\omega_{ph}^2(\mathbf{Q}) - i\omega\Gamma_{ph}(\mathbf{Q}) - \omega^2} \right) \quad (23)$$

where $\hbar\mathbf{Q} = \hbar(\mathbf{k}_f - \mathbf{k}_i)$ and $\hbar\omega$ are respectively the momentum and energy transfer of the scattering process, $n(\omega)$ the Bose-Einstein factor, which, in most of the energy range, can be

approximated by $\frac{kT}{\hbar\omega}$, $F(\mathbf{Q})$ is the static structure factor, $\omega_{\text{ph}}^2(\mathbf{Q})$ the (temperature dependent) phonon frequency and $\Gamma_{\text{ph}}(\mathbf{Q})$ its damping parameter, equal to its FWHM for underdamped phonons.

b) A Lorentzian central peak representing the spin reorientation dynamics for some temperature and frequency range. This peak is expressed as

$$S_L(\mathbf{Q}, \omega) = (1 + n(\omega)) \frac{I_L(\mathbf{Q})}{\Gamma_L(\mathbf{Q})} \text{Im} \left(\frac{1}{1 - i\omega\Gamma_L(\mathbf{Q})} \right) \quad (24)$$

where $\Gamma_L(\mathbf{Q})$ is the HWHM of this central peak and $I_L(\mathbf{Q})$ its intensity at

$$\omega = 0.$$

c) A $\delta(\omega)$ peak, which takes into account the incoherent elastic scattering processes. This mechanism is always present in the experiments and should be essentially temperature independent.

All our data were systematically fitted, taking into account resolution effects. This was achieved by computing the total response function (sum of the three terms listed above) convoluted with the resolution of the spectrometer. Least square refinements of the raw data provided, for each temperature and wave vector, I_L , Γ_L , ω_{ph} , Γ_{ph} , $F(\mathbf{Q})$, as well as the Dirac peak intensity and we verified that, for each \mathbf{q} , the latter did not depend on temperature, as expected. Let us finally note that even though we used a good energy resolution, we could not avoid, for very small momentum transfer, contamination effects arising from the nearby Bragg peak.

4.3 EXPERIMENTAL RESULTS.

4.3.1 Atmospheric pressure results. — The mode which propagates along \mathbf{c}^* and is polarized along \mathbf{b} is not coupled to the pseudospin variables. It was thus expected to be temperature insensitive, and to have a narrow linewidth at any temperature. This last point is well exemplified in figure 2 which shows the corresponding data at 166 K for $\mathbf{q} = 0.2 \mathbf{c}^*$ and $\mathbf{q} = 0.3 \mathbf{c}^*$. The line width of the phonon is indeed quite narrow (e.g. 0.044 ± 0.005 THz at $\mathbf{q} = 0.2 \mathbf{c}^*$ (0.18 \AA^{-1})).

In the (010) scattering plane, the two purely transverse acoustic modes propagating along \mathbf{c}^* and \mathbf{a}^* have been observed near the (400) and the (002) Bragg reflections, respectively. The two branches have been obtained at different temperatures in the range 300 K – 166 K. The results demonstrate that they have the same behaviour. In figure 3, we show some data relative to the mode which propagates along \mathbf{c}^* at $\mathbf{q} = 0.1 \mathbf{c}^*$ (0.09 \AA^{-1}). The phonon is clearly seen to soften when the temperature decreases from 252 K to 172 K and it becomes overdamped near the phase transition. ($\Gamma = 0.43 \pm 0.04$ THz at 172 K). The central part of the scan ($\omega = 0$) is the elastic incoherent response of the crystal. The full line indicates the result of a least square fit following the procedure explained above, and does not contain any Lorentzian contribution.

This softening is further exemplified in figure 4 where are represented as a function of temperature, the square of the phonon frequencies for approximately equal values of \mathbf{q} along \mathbf{c}^* and \mathbf{a}^* for the two cases: $\mathbf{q} = 0.05 \mathbf{c}^*$, and $0.1 \mathbf{a}^*$ ($q \sim 0.05 \text{ \AA}^{-1}$) and $\mathbf{q} = 0.1 \mathbf{c}^*$ and $0.2 \mathbf{a}^*$ ($q \sim 0.1 \text{ \AA}^{-1}$).

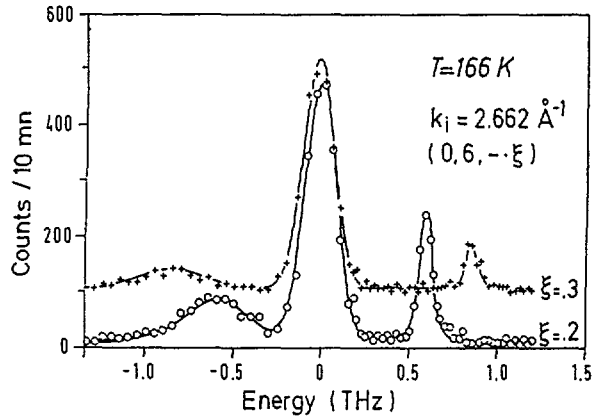


Fig. 2. — Neutron scans at $P = 0$ kbar and $T = 166$ K for $q = 0.2 c^*$ and $q = 0.3 c^*$ in the (100) plane, exhibiting the narrow TA phonons polarized along b .

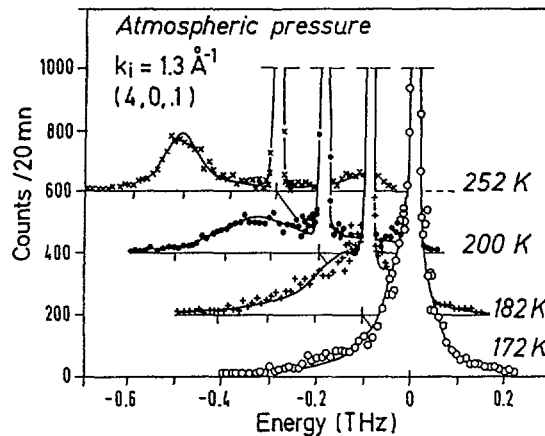


Fig. 3. — Neutron scans at $P = 0$ kbar and $q = 0.1 c^*$ at various temperatures for a scattering vector in the (010) plane, exhibiting broad TA phonons polarised along a . The full line is the convolution of the instrumental resolution function with a damped oscillator plus a $\delta(\omega = 0)$ incoherent elastic peak.

4.3.2 5 kbar results. — High pressure was generated in an aluminium alloy cell with helium as pressure medium. Pressure is determined with a precision of ± 10 bar. As at atmospheric pressure, the measurements were performed on the purely transverse acoustic branches of the (010) plane as a function of temperature, limiting here the range from 200 K to 138 K which is the phase I-III transition temperature. Many data were collected in the vicinity of $q = 0.17 c^*$ where the satellite will eventually appear below T_c , in order to analyse properly the dynamics of the transition.

Figure 5 displays the data for $q = 0.1 c^*$. At this pressure, the fitted results demonstrate that the phonon frequency remains temperature independent ($\omega_{ph} \simeq 0.27$ THz) while its damping slightly increases with decreasing temperature. At the same time, a central response is shown

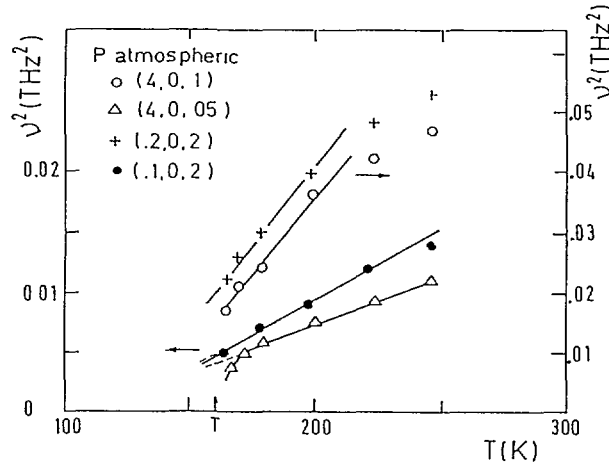


Fig. 4. — Square of the phonon frequencies at $P = 0$ kbar for $\mathbf{q} = 0.05 \mathbf{c}^*$ and $0.1 \mathbf{a}^*$ (left scale) and $0.1 \mathbf{c}^*$ and $0.2 \mathbf{a}^*$ (right scale), versus temperature. Note the downwards curvature of the curves.

to develop with decreasing temperature. Its profile has been fitted by a Lorentzian function, the half width at half maximum of which decreases while its intensity increases. These may be compared to those of figure 3: in particular, one sees that, 15 K above the transition at atmospheric pressure, the mode has softened to 0.16 THz ($T \simeq 182$ K) and the $\omega = 0$ resonance is only the δ elastic incoherent response; conversely, at 5 kbar and 143 K, i.e. 5 K only above the transition, the mode frequency is still 0.27 THz but the $\omega = 0$ part of the scan has no δ profile.

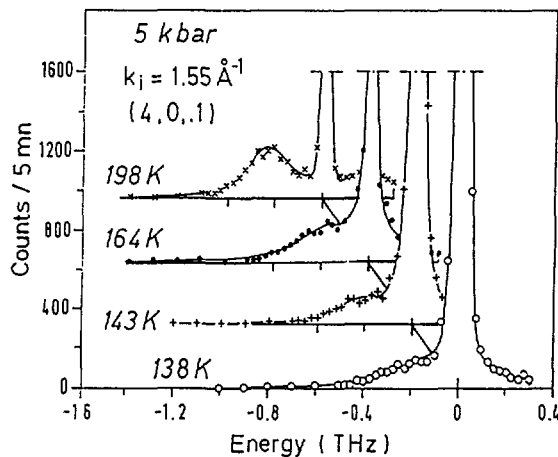


Fig. 5. — Same as in figure 3 at $P = 5$ kbar. A Lorentzian central peak has been added to the incoherent peak and the damped oscillator before convolution with the instrumental resolution function.

5. Discussion.

5.1 QUALITATIVE DISCUSSION. — Let us first proceed to a semi qualitative discussion of the experimental results by comparing the parameters obtained for the damped oscillator and for the central peak to the predictions of the model analysed in section 2, first at zero pressure, then at 5 kbar.

5.1.1 Zero pressure results. — As mentioned at the end of section 2, at zero pressure where the phase transition takes place at the Brillouin zone center, one expects that for low q values, the TA phonons both for $q \parallel c^*$, $u \parallel a$ and for $q \parallel a^*$, $u \parallel c$, will show typical soft mode behaviours: the phonon frequency decreases markedly when T decreases towards the critical temperature T_c and no central peak is detectable while, at each temperature, the phonon FWHM, increases as q^2 .

The first two results are clearly demonstrated by figures 3 and 4, and the straight lines of figure 4 show that the squares of the phonon frequencies do not follow, in the whole temperature range, a $(T - T_c)$ law; this is in agreement with equation (15), in which the first term of the r.h.s. has an hyperbolic dependence on temperature.

We have plotted in figure 6, $\sqrt{\Gamma(q)}$, the square root of the FWHM of the phonons for various values of $q \parallel c^*$ at $T = 242$ K, 198 K and 180 K. As expected from equation (15), for small values of q , $\sqrt{\Gamma(q)}$ is linear in q , the full curve having a downwards curvature, indicating that the $v_0 q \tau \ll 1$ condition is less and less fulfilled with increasing q . Furthermore, as τ is expected to increase with decreasing temperature, this condition should be limited to shorter values of q when the temperature decreases.

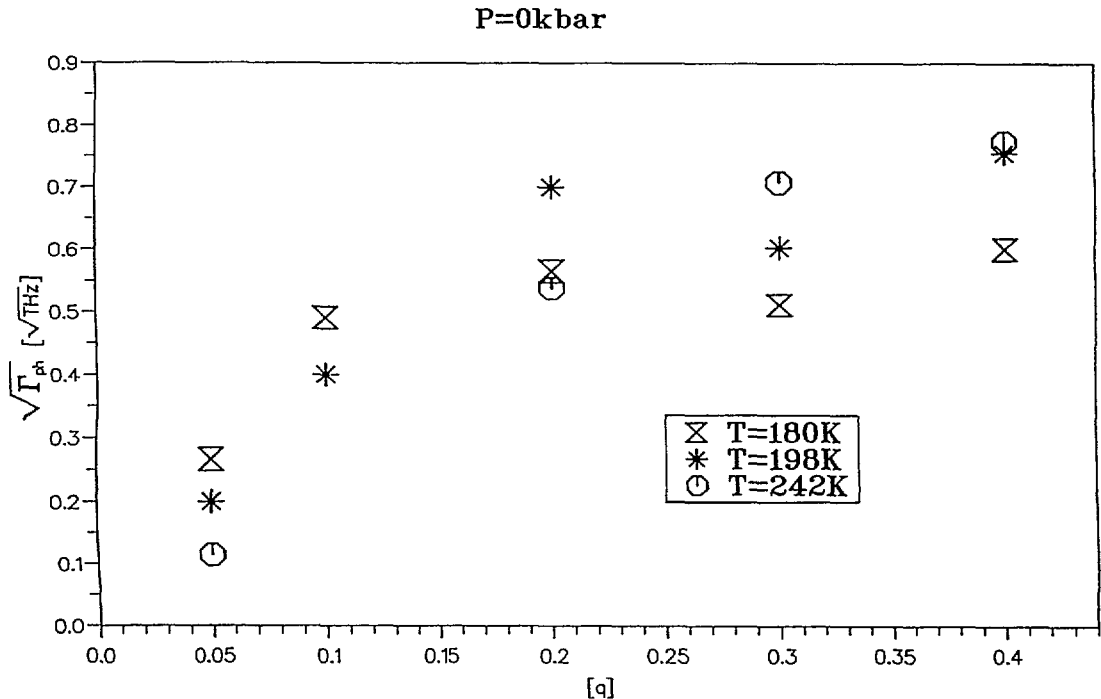


Fig. 6. — $\sqrt{\Gamma_{ph}(q)}$ versus q (in $|c^*|$ unit) for $q \parallel c^*$ and $P = 0$ kbar at $T = 242$ K, 198 K and 180 K.

This last effect is also apparent in figure 6: the domain of validity of the law $\sqrt{\Gamma(\mathbf{q})} \sim q$ is practically limited to $q \lesssim 0.1 \text{ c}^*$ at $T = 180 \text{ K}$ while it extends, at least, up to $q = 0.2 \text{ c}^*$ at $T = 242 \text{ K}$.

5.1.2 5 kbar results. — The shape of the response function is quite different from the zero pressure case, as was already apparent when comparing figures 3 and 5: at 5 kbar, no softening of the damped oscillator can be detected in the neutron data fit in the vicinity of $q_0 = 0.17 \text{ c}^*$, where the incommensurate satellite will eventually appear below T_c ; conversely, at each wave vector, a central ($\omega = 0$) peak develops with decreasing temperature.

These two results clearly appear in figures 7 and 9. A plot of the damped oscillator frequency, ω_{ph} , versus T is shown in figure 7 for $q = 0.15 \text{ c}^*$, 0.17 c^* and 0.20 c^* respectively. In each case, this frequency is essentially constant within experimental uncertainty, exhibiting in fact a small frequency increase with decreasing temperature which is beyond the approximations considered in this paper. The ($\omega = 0$) intensity of the central peak, I_L is reported, for the same values of q , in figure 9a while the corresponding HWHMs of this Lorentzian peak are shown in figure 9b: as expected, the central peak intensity increases with decreasing temperature, tending to diverge for $q = q_0$ and $T = T_c$, while its linewidth decreases, and tends to zero in the same limit, in agreement with equation (17).

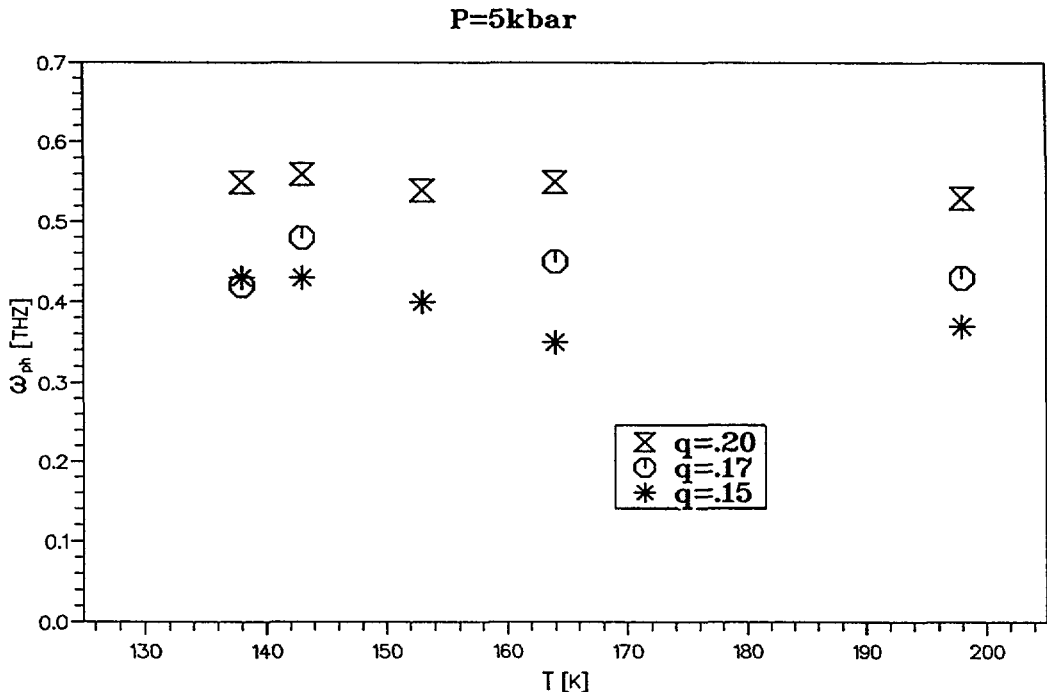


Fig. 7. — $\omega_{\text{ph}}(\mathbf{q})$ versus T at $P = 5 \text{ kbar}$ for $q = 0.15 \text{ c}^*$, 0.17 c^* and 0.20 c^* .

The model analysed in section 2 also predicts the damped phonon linewidth to be, at each temperature, wave vector independent in the $v_0 q \tau \gg 1$ regime (Eq. (16b)), and this result should be more valid, the larger the q . Figure 8 on which Γ_{ph} is plotted versus q for $T = 198 \text{ K}$,

152 K and $T = 138$ K, is, from this point of view, rather disappointing. It shows both a large scattering of the results (see, e.g., the two low temperature values) and no real tendency to saturation for large q , even if one is very far from the $\Gamma \sim q^2$ regime of the $P = 0$ kbar results, and if the damped oscillator linewidths are, as anticipated, much larger at $P = 5$ kbar than at 0 kbar for each value of q and T .

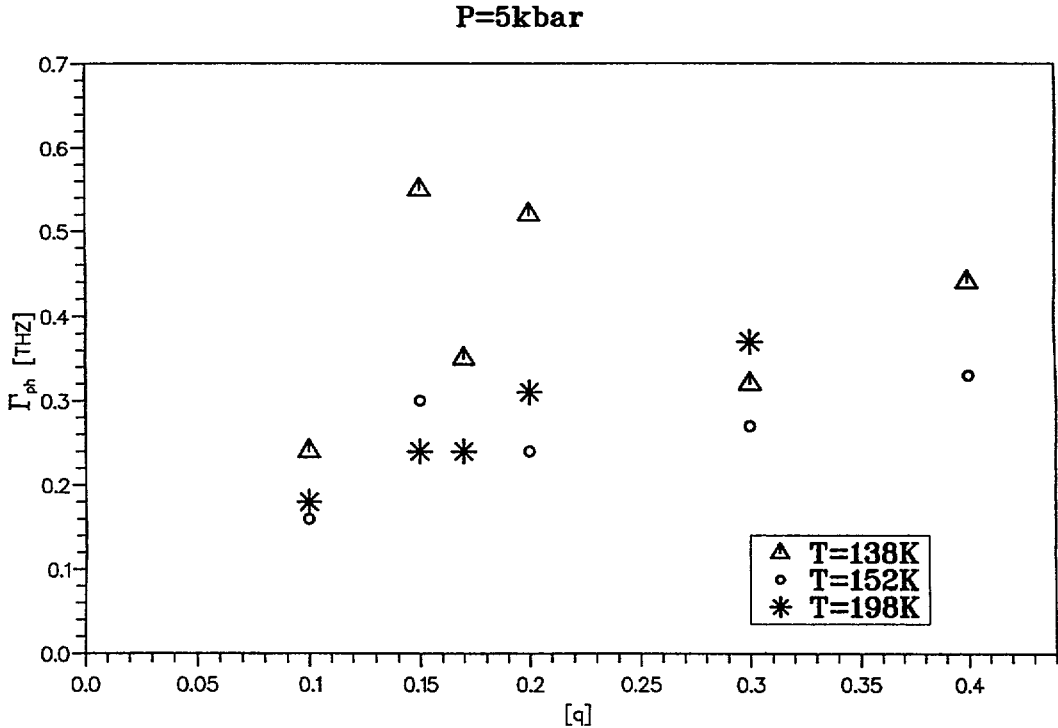


Fig. 8. — $\Gamma_{ph}(q)$ versus q at $P = 5$ kbar for $T = 198$ K, 152 K and 138 K.

5.2 GLOBAL FIT OF THE DATA. — The previous results show that the parameters obtained by the fitting procedure of section 4 qualitatively behave as predicted by the model in section 2, indicating the validity of the pseudospin acoustic phonon coupling hypothesis. Nevertheless our fitting procedure has treated each temperature and each wave vector independently. Due to the weak intensity of many spectra, this technique introduces large statistical errors: for instance, in figure 9, the intensity of the central peak at 138 K is higher at $q = 0.15$ c^* than at $q = 0.17$ c^* , contrary to what is expected. This prevents those parameters to be further analysed with the help of the various expressions derived in that section. In order to test more carefully the validity of our model, we have, in a second step, proceeded to a global fit of all the data pertinent to a given pressure. Considering that the spectral profiles, as obtained in section 4, represent a first approximation of the global phonon response function (Eq. (14)), we have looked for the values of v_o , d , $T_d(q)$ and $\tau(T)$ which give an overall best fit to the spectral profiles collected at different wave vectors and temperatures for a given pressure. Due to equations (1), (13) and (18), this yields at 0 kbar, seven independent parameters: τ_o and

V_0 which define $\tau(T)$, A , B , C and K which characterize $T_d(\mathbf{q})$ and, finally, v_0 , the sound velocity. At 5 kbar, the number of independent parameters reduces to six, as A , B and K are coupled through

$$C - B = 4K \cos \mathbf{q}_0 \cdot \frac{\mathbf{c}}{2} \quad (25)$$

while $\mathbf{q}_0 = 0.17 \mathbf{c}^*$ is experimentally determined.

The global fits have been performed using all the spectra collected at a given pressure. In both cases, these spectra correspond to \mathbf{q} along \mathbf{a}^* and \mathbf{c}^* , sampling more closely the vicinity of \mathbf{q}_0 ($= 0$ at 0 kbar or $0.17 \mathbf{c}^*$ at 5 kbar). 39 spectra were used at both pressures with temperatures ranging from 295 K to 163 K at 0 kbar, and from 198 K to 136 K at 5 kbar.

The seven parameters resulting from these global fits are given in table I for both pressures. Our results are also graphically displayed in figure 10 which represents $T_d(\mathbf{q})$ for $\mathbf{q} \parallel \mathbf{a}^*$ and $\mathbf{q} \parallel \mathbf{c}^*$ at 0 kbar (Fig. 10a) and 5 kbar (Fig. 10b) while the residence time, τ , is plotted versus T for those two pressures in figure 11. Let us comment on the values of these parameters.

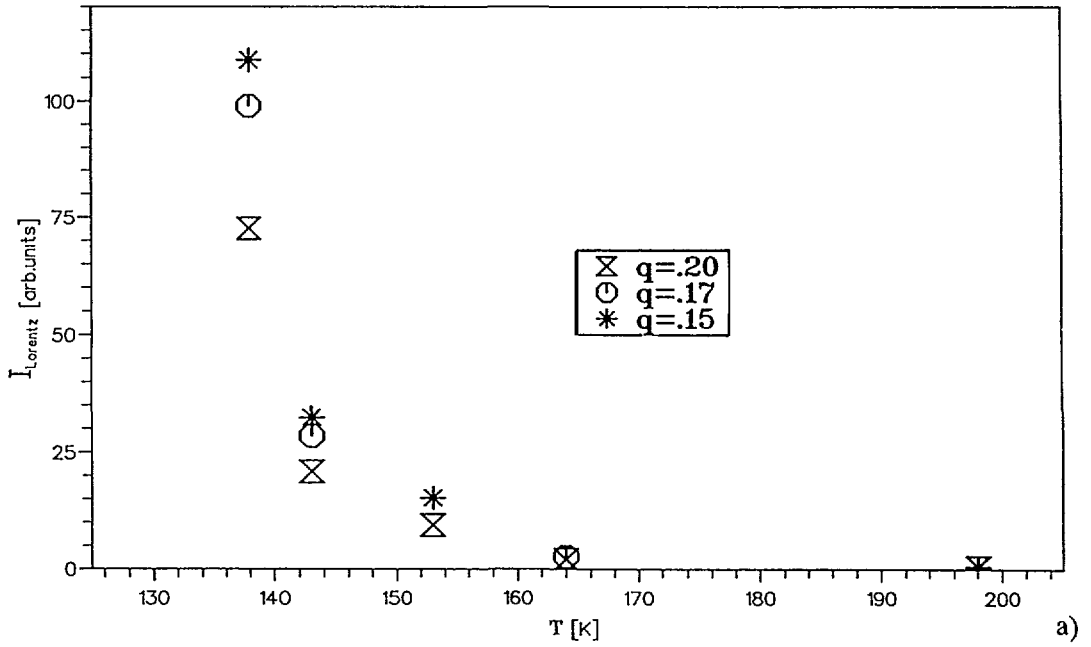
Table I. — Values of the parameters entering into the acoustic response function at $P = 0$ kbar and 5 kbar. τ_0 is in pcs, V_0 , A , B , C and K are in Kelvin, $\frac{v_0}{c}$ is in THz, where v_0 is a sound velocity, and c is the lattice parameter in the c direction.

	0 kbar	5 kbar
τ_0	0.05 ± 0.02	0.035 ± 0.012
V_0	302 ± 83	398 ± 51
A	39 ± 20	53 ± 20
B	-60 ± 20	-90 ± 30
C	67 ± 20	68 ± 22
K	24 ± 13	46 ± 8
$\frac{v_0}{c}$	3.1	3.4

For zero pressure, $T_d(\mathbf{q} = 0)$ is reasonably close to its hydrogenated value ($T_d(\mathbf{q} = 0) = 40$ K) [5]; similarly, the barrier energy V_0 is 302 K for AHOD instead of 320 K for AHO, and the individual residence time, τ , measured at 250 K is 0.17 pcs in AHOD instead of 0.15 pcs in AHO. The values relative to the NH_4^+ or ND_4^+ reorientations are thus comparable for AHOD and AHO at zero pressure, which is already a satisfactory result as the techniques used here and in [5] are quite different.

Another important test of our model consists in comparing the 0 kbar and 5 kbar values of the different parameters. They turn out to be, as expected, in agreement. The speed of sound, v_0 , differs by less than 10 percent between these two pressures, and the different parameters describing the various interactions between the pseudospins are only moderately affected by the application of pressure. Furthermore, for both pressures, there is clear dependence of $T_d(\mathbf{q})$ on \mathbf{q} for $\mathbf{q} \parallel \mathbf{a}^*$. Nevertheless, as is apparent in figures 10a and b, these small changes, and in particular the larger increase of K with respect to $C - B$, are sufficient to shift the maximum of $T_d(\mathbf{q})$ from $\mathbf{q} = 0$ at zero pressure to $\mathbf{q} = 0.17 \mathbf{c}^*$ at 5 kbar. This does not affect substantially the value of the maximum of $T_d(\mathbf{q})$: the 5 kbar pressure is too close to the critical pressure P_c to make an important change on the maximum value of the interaction constant.

P=5kbar



P=5kbar

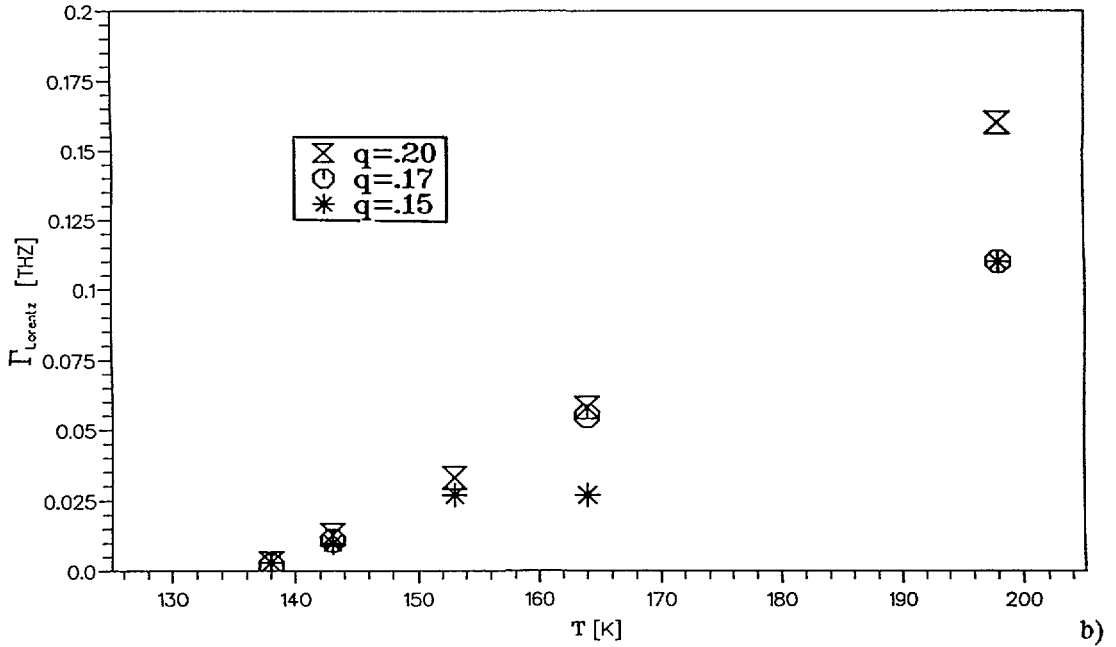


Fig. 9. — $I_L(q)$ (a) and $\Gamma_L(q)$ (b) versus T at $P = 5$ kbar.

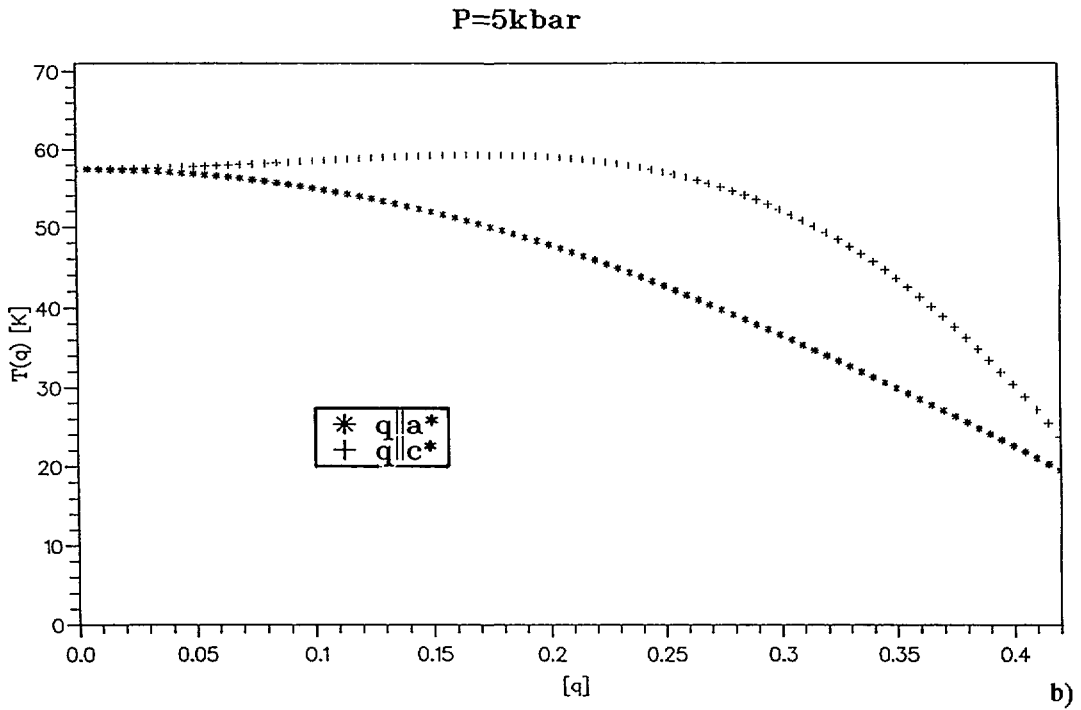
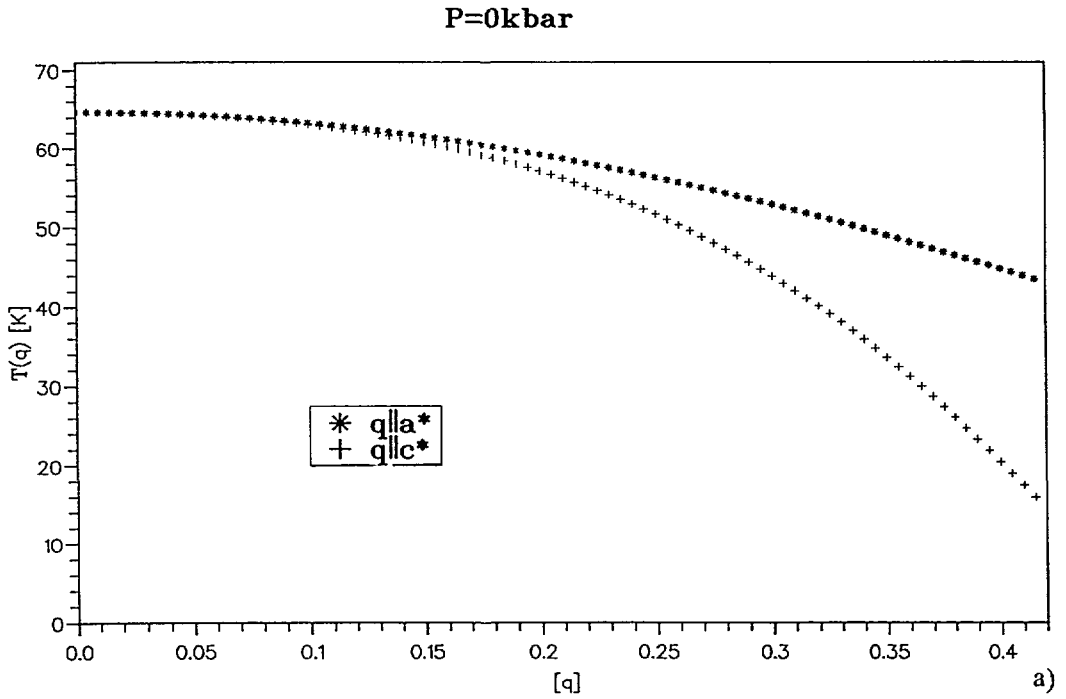


Fig. 10. — $T_d(\mathbf{q})$ at $P = 0$ kbar (a) and 5 kbar (b) for $\mathbf{q} \parallel \mathbf{c}^*$ and $\mathbf{q} \parallel \mathbf{a}^*$ in units $|\mathbf{c}^*|$ or $|\mathbf{a}^*|$ respectively.

Another important aspect, is the increase of both τ_0 and V_0 with pressure. As expected, it reduces very much the $T - q$ domain in which, for the TA phonon, $\omega_{ph}\tau < 1$. For instance, for $q = 0.1 \text{ c}^*$, while this condition is always fulfilled at zero pressure, it is only fulfilled, at 5 kbar, above 180 K, and it is never the case, at this pressure, for $q = 0.17 \text{ c}^*$. This explains the large difference appearing, for instance, between the spectra shown in figures 3 and 5.

Let us finally note that the analysis which we performed has been based on extremely severe conditions: for instance, a linear dispersion relation for all the acoustic phonons considered here may be an over simplification, as well as the total independence of the corresponding speed of sound on temperature. The quality of the global fits could have been largely improved by taking such effects into account, as well as by adding an intrinsic acoustic phonon linewidth due to the orientational disorder existing in AHOD. As the major objective of this paper was to test the effect of applying pressure on the coupled phonon-pseudospin statics and dynamics, we have decided to stick to the minimum of meaningful parameters, the various uncertainties coming from their increased number making more hazardous any quantitative discussion.

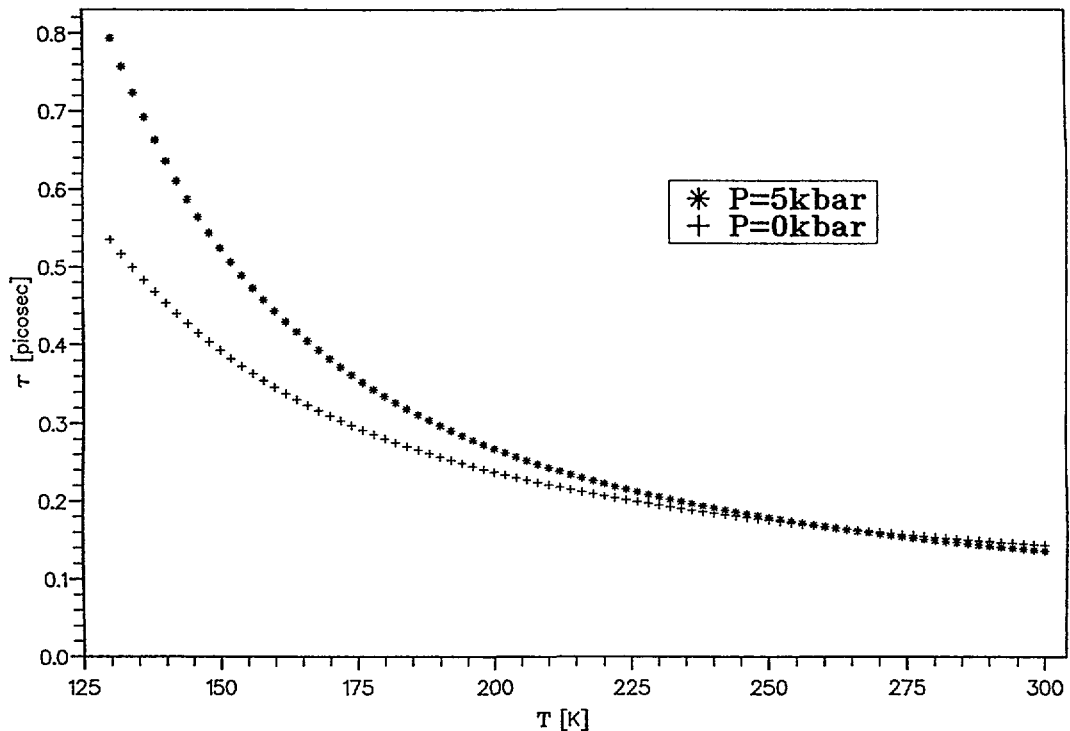


Fig. 11. — Residence time τ , versus temperature for $P = 0$ kbar and 5 kbar.

6. Summary. Discussion. Concluding Remarks.

In the present paper, we have analysed a neutron inelastic coherent scattering experiment performed on AHOD, at zero pressure and at 5 kbar, in the high temperature disordered phase.

This experiment was designed to test the validity of a model for the series of phase transitions which take place in this crystal. This model explains these transitions as the result of a linear coupling between one specific linear combination of the pseudospin variables describing the orientational disorder of some ND_4^+ ions on the one hand and a transverse acoustic phonon on the other hand. This phonon either propagates along c^* and is polarized along a , for $P > P_c$, or is its $q \rightarrow 0$ limit, i.e. the e_5 deformation, for $P < P_c$.

We have shown that this model correctly explains the data collected in our experiments both above P_c (5 kbar experiments) and at zero pressure. The static change from a zone center transition to a normal-incommensurate transition has been described as the result of an ANNNI model i.e. a competition between nearest neighbouring planes of ND_4^+ with ferro-type pseudospin interactions and an antiferro-type of interaction between second nearest planes. A weak evolution of these interactions with pressure is sufficient to change the transition from a ferroelastic to an incommensurate one.

As for the dynamics of the transition, it is governed by the individual pseudospin reorientation motions. As could be anticipated from steric hindrance considerations, the application of pressure increases the residence time of the individual ND_4^+ ions at the bottom of their orientational well. Consequently, the dynamics changes from a soft mode behaviour at zero pressure to a hard mode plus a dynamical central peak description at 5 kbar, the acoustic phonon frequency being hardly affected by the approach of the phase transition. The only effect on the TA phonons is, in this case, an increase of their linewidths, due to the linear coupling to the pseudospin dynamics.

Recently, Poon [16] proposed a somewhat different mechanism to describe the series of phase transitions which take place in AHO or AHOD, based on an original idea of Heine and Mc Connell [17-18]. Noting, from dielectric measurements performed by Albers and Küppers [15] on AHO, that the xx component of its dielectric tensor, $\epsilon_{xx}(T)$, exhibits above T_c , at zero pressure, a Curie-Weiss behaviour with a Curie temperature of approximately -20 K, Poon concluded to the existence of a "mode" with B_{3u} symmetry, which would freeze by itself at such a temperature. He also noted that, along c^* , both B_{2g} and B_{3u} representations give rise to the same τ_4 representation. Following the ideas of [18], the B_{2g} "mode" which actually freezes at 0 kbar, and the B_{3u} mode are 90° out of phase and couple, along c^* , through a coefficient the leading term of which is proportional to q . Those modes could be the set of two deformations which realize a compromise of the free energy when an incommensurate phase is formed [18]. Poon proposed that, among these two soft modes, the frequency of the B_{3u} mode would decrease with increasing pressure, while the B_{2g} mode would not depend on pressure. He showed that, within such a model, the application of pressure would lead to a normal-incommensurate phase transition with a vector q_0 parallel to c^* above a critical pressure. The present results, though they do not rule out some aspects of Poon's mechanism, are not in favour of most of the points made in [16].

Let us first note that Albers and Küppers measurements agree with the model developed here: as was already shown in [5], the four pseudospins contained in the high temperature unit cell generate, at $q = 0$, four variables belonging to four different irreducible representations. One is in the B_{2g} representation, which dynamics has been studied in [5] and in this paper; a second is in the B_{3u} representation and is responsible for the results reported in [15]; a third is in the B_{1g} representation, active in Raman spectroscopy and its dynamics was also detected in [5], while the last, A_u representation is silent in all these techniques. Each of these variables has its own freezing temperature, in agreement with [16], though their dynamics are diffusive, and not propagative as suggested by Poon.

Nevertheless, as can be inferred from section 3, the interactions between these modes at any point in the Brillouin zone have the same origin as the q dependence of $J_d(q)$, namely the

individual pseudospin interactions. Each of them varies with pressure, as we have seen in the present study, and one cannot assume that the pseudospin variable originated from the B_{3u} representation is more pressure sensitive than any other.

One may also analyse, within the interaction model developed in section 3, what would be the effect of taking into account Poon's type of coupling. In the language of section 2, $\sigma_a(\mathbf{q})$ is the variable which transforms as B_{3u} at $\mathbf{q} = 0$, and the calculation which leads to equation (18) can be extended to include in the pseudospin free energy $\sigma_d(\mathbf{q})$, $\sigma_a(\mathbf{q})$ and their linear coupling. If, following [16], one eliminates, in an adiabatic approximation, the $\sigma_a(\mathbf{q})$ variable, and considers that the $\sigma_a(\mathbf{q})$ freezing temperature is well below the temperatures used in the present experiments, (an approximation which agrees with the numerical values of Tab. II) one ends up (cf. Annex A) with an additional term in $J_d(\mathbf{q})$ which reads:

$$\frac{B'^2}{k_B T} \sin^2 Z \equiv \frac{B'^2}{2k_B T} (1 - \cos 2Z) \quad (26)$$

where B' is an interaction constant similar to B but related to a difference of energy between pseudospins. The mechanism considered by Poon gives thus, as could be anticipated, a contribution analogous to that given by the interaction between the pseudospins separated by $\pm c$, the only difference being its additional weak temperature variation. But no term proportional to $\cos Z$, and/or to $\cos X$, can be obtained from such a mechanism, and such terms are necessary to produce the maximum along c^* , and the dispersion along a^* . Our experiments cannot rule out a term like equation (26), which is at variance with (or in addition to) the mechanism represented by the interaction constant K , though the coefficient B' , which is a difference of interaction energies, is presumably smaller than the coefficient K which is a sum of such interaction energies.

Let us finally remark that, in the present paper, no attempt has been made to look at the dynamics of the system in the incommensurate phase. Some of us have recently studied it, in AHOD, by Raman spectroscopy [18]. This gives information only for the $\mathbf{q} = \mathbf{o}$ wave vectors but generates spectral profiles of much better accuracy, and also allows one to study the pseudospin dynamics related to the $\mathbf{q} = \mathbf{o}$, B_{1g} mode. The results of both techniques are in good agreement, and the trends found in this study when passing from zero to five kbars have also been confirmed.

Acknowledgements.

We would like to thank Mr J.M. Godard who has grown the AHOD crystal at Orsay University for us, Dr B. Hennion from L.L.B. for his constant help while using the neutron deconvolution program, as well as Mrs A. Colline, Dr D. Kirin and Dr N. Toupry for their contribution while fitting the neutron data with the present model. This work was partly supported by the Scientific Affairs Division of NATO, through grant N° 86-0283.

Appendix.

In the interaction energy model described in section 3, there exist two types of energy terms. The first one contains the interactions between pseudospins separated, either by $\pm c$, or by $\simeq \left(\pm \frac{a}{2} \pm \frac{c}{2}\right)$: in both cases, the interaction between one ND_4^+ and each of its neighbours can be deduced from one of them by space group operations. One can verify that, in such a case,

the interaction energy diagonalizes, whatever is \mathbf{q} , into the four variables $\sigma_a(\mathbf{q})$, $\sigma_b(\mathbf{q})$, $\sigma_c(\mathbf{q})$ and $\sigma_d(\mathbf{q})$ given by equation (7).

The second type is related to the interactions between one pseudospin and its neighbours contained in planes differing by $\simeq \pm \frac{\mathbf{b}}{2}$. There, the space group operations do not transform one pair of pseudospins (e.g. separated by $\sim \frac{\mathbf{a} + \mathbf{b}}{2}$) into the four pairs separated by $\sim \left(\pm \frac{\mathbf{a}}{2} \pm \frac{\mathbf{b}}{2} \right)$, but only into two of them, and the same is true for the pairs separated by $\sim \left(\frac{\mathbf{b} + \mathbf{c}}{2} \right)$. For general values of \mathbf{q} , the interaction energy does not diagonalize any longer into the four pseudospin variables.

When one restricts \mathbf{q} to the (010) plane, the only coupling which remains between the pseudospin variables is related to the non equivalence between the interaction energies of two pseudospins separated by $\simeq \frac{\mathbf{b} + \mathbf{c}}{2}$ and $\simeq \frac{\mathbf{b} - \mathbf{c}}{2}$. Let us call $2B'$ the difference between the two interaction constants (while $2B$ is their sum). Group theory easily shows that, in this (010) plane, $\sigma_d(\mathbf{q})$ couples only to $\sigma_a(\mathbf{q})$ and $\sigma_b(\mathbf{q})$ to $\sigma_c(\mathbf{q})$. If one restricts the free energy to the two first variables, one finds after an easy but lengthy calculation:

$$F_{ps} = \frac{1}{2} \sum_{\mathbf{q}} [(k_B T - J_d(\mathbf{q})) \sigma_d(\mathbf{q}) \sigma_d(-\mathbf{q}) + (k_B T - J_a(\mathbf{q})) \sigma_a(\mathbf{q}) \sigma_a(-\mathbf{q}) - (J_{ad}(\mathbf{q}) \sigma_a(\mathbf{q}) \sigma_d(-\mathbf{q}) + c.c.)] \quad (\text{A.1})$$

where $J_d(\mathbf{q})$ is given by equations (18) and (19),

$$J_a(\mathbf{q}) = A \cos X + B \cos Z + C \cos X \cos Z - K \cos 2Z, \quad (\text{A.2})$$

$$J_{ad}(\mathbf{q}) = iB' \sin Z, \quad (\text{A.3})$$

A , B , C and K being defined below equation (19).

Equation (A.3) shows that the coupling between $\sigma_a(\mathbf{q})$ and $\sigma_d(\mathbf{q})$ disappears for $\mathbf{q} \parallel \mathbf{a}^*$ in agreement with the fact that the two variables belong respectively to the τ_1 and τ_3 representations in this case.

In the adiabatic approximation considered by Poon, one writes:

$$\frac{\partial F}{\partial \sigma_a(-\mathbf{q})} = 0 \quad (\text{A.4})$$

which gives a linear relation between $\sigma_d(\mathbf{q})$ and $\sigma_a(\mathbf{q})$. Neglecting $|J_a(\mathbf{q})|$ with respect to $k_B T$, and eliminating $\sigma_a(\mathbf{q})$ through equation (A.4), equation (A.1) simplifies into

$$F'_{ph} = \frac{1}{2} \sum_{\mathbf{q}} \left(k_B T - J_d(\mathbf{q}) - \frac{B'^2 \sin^2 Z}{k_B T} \right) \sigma_d(\mathbf{q}) \sigma_d(-\mathbf{q}). \quad (\text{A.5})$$

References

- [1] KUPPERS H., *Acta Cryst.* **A28** (1972) 522.
- [2] KUPPERS H., *Acta Cryst.* **B29** (1973) 318.
- [3] KELLER H.L., KUCHARCZYK D. and KUPPERS H., *Z. Kristallogr.* **158** (1982) 221.
- [4] BENOIT J.P., BERGER J., KRAUZMAN M. and GODET J.L., *J. Phys. France* **47** (1986) 815.
- [5] GODET J.L., KRAUZMAN M., MATHIEU J.P., POULET H. and TOUPRY N., *J. Phys. France* **48** (1987) 809.
- [6] GODET J.L., Thesis, Université Pierre et Marie Curie, Paris (1985) unpublished
- [7] GODET J.L., KRAUZMAN M., PICK R.M., POULET H. and TOUPRY N., *J. Phys. France* **50** (1989) 1711.
- [8] BOSIO L., OUMEZZINE M. and PICK R.M., *Revue Phys. Appl.* **23** (1988) 105.
- [9] KRAUZMAN M., GODET J.L., PICK R.M., POULET H., TOUPRY N., BOSIO L., DEBEAU M., LAUNOIS P. and MOUSSA F., *Europhys. Lett.* **6** (1988) 374.
- [10] KUPPERS H., *Z. Kristallogr.* **140** (1974) 393.
- [11] YAMADA Y., TAKATERA H. and HUBER D.L., *J. Phys. Soc. Jap.* **36** (1974) 641.
- [12] KOVALEV O.V., Irreducible representations of the space groups, (Gordon and Breach, New York, 1965).
- [13] ROWE J.N., RUSH J.J., CHESSER N.J., MICHEL K.H. and NAUDTS J., *Phys. Rev. Lett.* **40** (1978) 455.
- [14] SELKE W., *Phys. Rep.* **170** (1988) 213.
- [15] ALBERS J. and KUPPERS H., *Phys. Status Solidi* **a39** (1977) K49.
- [16] POON W.C.K., *J. Phys.: Cond. Matter* **2** (1990) 10249.
- [17] HEINE V. and Mc CONNELL J.D.C., *Phys. Rev. Lett.* **46** (1981) 1092.
- [18] HEINE V. and Mc CONNELL J.D.C., *J. Phys. C: Solid State Phys.* **17** (1984) 1199.
- [19] KRAUZMAN M., COLLINE A., KIRIN D., PICK R.M. and TOUPRY N., to be published.

Revue de livres

Three hundred years of gravitation

S. W. HAWKING et W. ISRAEL Eds.

(Cambridge University Press, 1987) 684 p., £ 45.00, \$ 69.50.

L'année 1987 a vu la commémoration du tricentenaire de la parution des « Principes mathématiques de la Philosophie Naturelle » d'Isaac Newton, en latin évidemment. Il était donc judicieux de réunir en un volume de bonne taille des essais mêlant l'histoire à la recherche contemporaine qui pour de nombreuses raisons — discutées par différents auteurs — a remis l'étude de la gravitation au premier plan. Lecteur de bonne volonté mais nullement averti j'avoue, après avoir feuilleté à de nombreuses reprises les quelques sept cents pages, être en difficulté pour en donner un compte rendu honnête tant la matière est dense et riche. Cependant nul ne peut ignorer ce sujet majeur et je suis sûr que quiconque ouvrira le livre trouvera matière à apprendre et à réfléchir. Il convient même brièvement d'énumérer les têtes de chapitres — chacun écrit par une autorité incontestable. Sans leur rendre la justice qu'il conviendrait, parcourons la table des matières.

L'ouvrage s'ouvre par une introduction historique de Hawking, un essai sur la « philosophie naturelle » de Weinberg, et une étude de Penrose sur la théorie corpusculaire de la lumière de Newton qui se poursuit par des spéculations sur la mécanique quantique, l'objectivité et la relativité générale. Les articles de Cook et Will sur les aspects expérimentaux sont passionnants en ce qu'ils révèlent combien il est difficile, encore aujourd'hui, de mettre à l'épreuve la relativité einsteinienne mais aussi bien les hypothèses fondamentales de la gravité newtonienne et j'avoue avoir découvert avec surprise que la constante de la gravitation n'est connue qu'avec une précision relative de 10^{-4} . T. Damour consacre un long essai aux très difficiles problèmes qui se posent pour mettre en œuvre des calculs en gravitation et en relativité générale tandis que W. Israel donne un exposé historique détaillé sur la matière noire et l'évolution des idées sur la topologie et la physique des trous noirs dont Blanford décrit les aspects expérimentaux. K. Thorne présente un panorama des essais — infructueux à ce jour — de mettre en évidence le rayonnement gravitationnel. La formation des galaxies est un sujet majeur en cosmologie discutée par Rees. La dernière série d'articles est plus spéculative, qu'il s'agisse du rôle possible des « cordes cosmologiques » (Vilmkin), du modèle d'inflation cosmologique (Blau et Guth, Linde), de la cosmologie quantique (Hawking) ou de la théorie des supercordes comme modèle unifié des interactions (Schwarz). Le dernier article, plus technique, de Crnkovic et Witten discute de la quantification en théorie de jauge et en relativité générale.

Après un tel menu on se persuade sans peine de l'ampleur du sujet dont la collection d'essais donne — ce me semble — un excellent panorama, et qui pourra servir de guide à qui désire approfondir l'un des multiples aspects. D'abondantes bibliographiques qui concluent chacun des chapitres seront très certainement très utiles ! En revanche, l'absence d'index général est regrettable. Dans le genre des ouvrages qui réunissent des auteurs variés, celui-ci paraît très réussi, sans compter qu'il rend pleinement hommage à l'un des plus grands physiciens, expérimentateur, théoricien et même mathématicien de génie.

En refermant le livre, on comprend pourquoi l'édifice dont Newton a posé les fondations suscite toujours un intérêt majeur et combien il reste à faire pour que la gravitation universelle s'accommode avec la géométrie de notre univers, des échelles les plus grandes, quelques milliards d'années lumières, aux plus courtes, cette mystérieuse longueur de Planck de quelques 10^{-33} cm. Recommandons sans hésiter des « trois cents ans de gravitation » aux chercheurs, astrophysiciens et physiciens, aux étudiants et même au public averti le plus large.

C. ITZYKSON (Saclay).

Schrödinger - Centenary celebration of a polymath

par C. W. KILMISTER, Ed.

(Cambridge University Press, 1987) 251 p., £ 12.50, \$ 22.95.

La personnalité de Schrödinger, né à Vienne en 1887 et mort à Alpbach dans le Tyrol en 1961, et la marque qu'il a laissée sur la physique du 20^e siècle justifiaient amplement la célébration d'un centenaire dont ce volume porte témoignage.

Qui s'intéresse à la personnalité d'un homme hors du commun et à sa vie mouvementée, lira avec intérêt l'introduction de Kilmister, éditeur du recueil, l'exposé de Flamm sur les influences qu'il a subies, en particulier celle de Boltzmann, et l'histoire des relations entre Schrödinger et E. de Valera qui l'attira en Irlande et créa pour lui le célèbre institut de Dublin, dans la description qu'en donne McCrea. Une biographie récente due à W. Moore et publiée par la même maison présente évidemment une vue plus approfondie de la carrière d'un scientifique exemplaire.

Le mot anglais « polymath » qui figure dans le titre et qu'on traduirait par « esprit encyclopédique », convient bien à Schrödinger. Ceci est reflété par la diversité des contributions.

Le livre s'ouvre par une étude de Dorling sur l'interprétation de l'équation de Schrödinger, équation d'onde qui dans l'esprit de son auteur tentait de donner un contenu plus concret aux abstractions de la mécanique des matrices de Heisenberg, Born et Jordan. On sait que Schrödinger — comme Einstein — eut ce destin étonnant d'un créateur qui ne parvint jamais à se réconcilier avec l'interprétation probabiliste et les discontinuités qu'introduit l'observation. Il n'est donc pas surprenant que l'article consacré à ce sujet par J. Bell — à son tour disparu — s'ouvre par une citation caractéristique de Schrödinger datant de 1952 et qu'on me permettra de reproduire : « If we have to go on with these damned quantum jumps, then I'm sorry that I ever got involved. »

C. N. Yang nous rappelle le rôle de l'arbitraire de phase des fonctions d'ondes complexes de la mécanique quantique que Schrödinger, dans la série de ses six articles mémorables de 1926, tentait vainement d'éviter (en considérant en particulier des situations stationnaires). On sait quel parti Weyl puis Yang plus tard tirèrent de cet arbitraire qui devait donner naissance à l'invariance de jauge.

Le rôle de l'équation d'onde en physique atomique et moléculaire, voire en physique des solides, est capital, qu'il s'agisse de la stabilité de la matière (Thirring), de la dynamique dans un contexte biomoléculaire (Karplus), des réactions chimiques (Fukui), de la chimie quantique (Buckingham).

On trouvera d'autres illustrations du développement de la mécanique quantique dans l'article de Lewis sur la condensation de Bose (reflétant les intérêts de Schrödinger pour la mécanique statistique), de Salam qui présente un panorama de la physique des particules, de Kibble qui décrit le rôle de la topologie en cosmologie, de Seaton sur les effets quantiques en astronomie, pour arriver à ce qui est peut-être la limite extrême lorsqu'il s'agit de la « fonction d'onde de l'univers » (S. Hawkins).

Ceci est l'occasion d'évoquer des travaux de Schrödinger qui n'eurent pas le succès espéré, comme ceux sur l'optique non linéaire (J. McConnell) ou sur les théories unifiées qu'il poursuivit sans résultat immédiat en parallèle avec Einstein (O. Hittmair).

L'une des grandes originalités de Schrödinger fut de s'intéresser très tôt à la biophysique. Son livre « What is Life » eut une profonde influence — que décrivent Pauling et Perutz (ce dernier un peu critique) — sur une génération entière.

De cette rapide description, on retiendra que les actes de ce colloque présentent un grand intérêt pour mesurer la postérité d'un des plus grands physiciens du siècle. Ils trouveront naturellement une place sur le rayon des bibliothèques consacré à l'évolution des idées scientifiques et leur lecture est vivement conseillée à tous les étudiants, enseignants et chercheurs.

C. ITZYKSON (Saclay).